

Stopping, Straggling, and Blooming of Directed Energetic Electrons in Hydrogenic Plasmas

A basic problem in plasma physics is the interaction and energy loss of energetic, charged particles in plasmas,^{1–3} including the effects of penetration, longitudinal straggling, and lateral blooming. This problem has traditionally focused on ions (i.e., protons, alphas, etc.), either in the context of heating and/or ignition in, for example, inertially confined plasmas (ICF)^{3–7} or the use of these particles for diagnosing implosion dynamics.⁸ More recently, prompted in part by the concept of fast ignition (FI) for ICF,⁹ studies have begun to consider energy deposition from relativistic fast electrons in deuterium–tritium (DT) plasmas.^{9–14} In this context, the mean penetration and stopping power for energetic electrons interacting with a uniform hydrogenic plasma of arbitrary density and temperature were recently calculated. Therein, the randomizing effect of electron scattering, which has a cumulative effect of bending the path of the electrons away from their initial direction, was linked to energy loss.¹⁴ This article presents calculations that show, for the first time, the effects of longitudinal straggling and transverse blooming and their inextricable relationship with enhanced electron energy deposition. It is demonstrated that, while the initial penetration results in approximate uniform energy deposition, the latter penetration has mutual couplings of energy loss, straggling, and blooming that lead to an extended region of enhanced, nonuniform energy deposition. This present work is important for quantitatively evaluating the energy deposition in several current problems. In the case of FI, for example, no evaluations have treated either straggling or blooming upon the energy deposition; without evaluation no confident assessment of ignition requirements can be made. Therefore, the calculations in this article form the foundation for a baseline, at the very least, or an accurate assessment, at the very most, by which to evaluate these effects upon fast ignition. In addition to FI, these calculations are, in general, sufficient to be of relevance to other current problems, such as fast-electron preheat¹⁵ in ICF, or to energy deposition of relativistic electrons in astrophysical jets.¹⁶

To delineate these processes, we calculate the different moments by analytically solving an integro-differential diffusion equation,¹⁷ thereby rigorously determining the angular and spatial distributions of the scattered electrons:

$$\frac{\partial f}{\partial s} + \mathbf{v} \cdot \nabla f = n_i \int [f(\mathbf{x}, \mathbf{v}', s) - f(\mathbf{x}, \mathbf{v}, s)] \sigma(|\mathbf{v} - \mathbf{v}'|) d\mathbf{v}', \quad (1)$$

where $f(\mathbf{x}, \mathbf{v}, s)$ is the distribution function, n_i is the number density of fully ionized plasma ions of charge Z , \mathbf{x} is the position where scattering occurs, $\sigma = \sigma_{ei} + Z\sigma_{ee}$ is the total scattering cross section with σ_{ei} the Rutherford e -ion cross section¹⁸ and σ_{ee} the Møller e - e cross section.¹⁹ We solve this equation in cylindrical coordinates with the assumption that the scattering is azimuthally symmetric. After expanding the distribution in spherical harmonics and substituting into Eq. (1), two differential equations for the longitudinal and lateral distributions are obtained. For the longitudinal distribution,

$$\frac{\partial F_{\ell m}^n(s)}{\partial s} + \kappa_{\ell}(s) F_{\ell m}^n(s) - n \left[\frac{\ell}{\sqrt{4\ell^2 - 1}} F_{\ell-1, m}^{n-1}(s) + \frac{\ell+1}{\sqrt{4(\ell+1)^2 - 1}} F_{\ell+1, m}^{n-1}(s) \right] = 0, \quad (2)$$

and for the lateral distribution,

$$\begin{aligned}
 & \frac{\partial F_{\ell m}^n(s)}{\partial s} + \kappa_{\ell}(s) F_{\ell m}^n(s) \\
 & - \frac{n}{2} \left[\sqrt{\frac{(\ell+m)(\ell+m-1)}{4\ell^2-1}} F_{\ell-1, m-1}^{n-1}(s) \right. \\
 & + \sqrt{\frac{(\ell+m+2)(\ell+m+1)}{4(\ell+1)^2-1}} F_{\ell+1, m+1}^{n-1}(s) \\
 & - \sqrt{\frac{(\ell-m)(\ell-m-1)}{4\ell^2-1}} F_{\ell-1, m+1}^{n-1}(s) \\
 & \left. - \sqrt{\frac{(\ell-m+2)(\ell-m+1)}{4(\ell+1)^2-1}} F_{\ell+1, m+1}^{n-1}(s) \right] = 0, \quad (3)
 \end{aligned}$$

where the moments are defined as

$$F_{\ell m}^n(s) = \int_{-\infty}^{\infty} x_j^n f_{\ell m}(\mathbf{x}, s) d\mathbf{x} \quad (4)$$

and $j=1, 2, 3$ represents x, y, z , respectively.

$$\kappa_{\ell}(s) = n_i \int \left(\frac{d\sigma}{d\Omega} \right) [1 - P_{\ell}(\cos\theta)] d\Omega, \quad (5)$$

where $P_{\ell}(\cos\theta)$ is the Legendre polynomial and $\kappa_{\ell}(s)$ is directly related to the basic transport cross section.² Equations (2) and (3) are coupled to adjacent orders in n and are solved with the boundary condition

$$F_{\ell m}^n(s) = \sqrt{\frac{2\ell+1}{4\pi}} \delta_{m0} \delta_{n0} \exp \left[- \int_0^s \kappa_{\ell}(s') ds' \right], \quad (6)$$

where $F_{\ell m}^n(0) = 0$ for $n \neq 0$. Solving for κ_1 and κ_2 ,

$$\kappa_1 = 4\pi n_i \left(\frac{r_0}{\gamma\beta^2} \right)^2 \left\{ Z^2 \ln \Lambda^{ei} + \frac{4(\gamma+1)^2}{\left[2^{\sqrt{(\gamma+1)/2}} \right]^4} Z \ln \Lambda^{ee} \right\}; \quad (7)$$

and

$$\kappa_2 = 12\pi n_i \left(\frac{r_0}{\gamma\beta^2} \right)^2 \times \left\{ Z^2 \left(\ln \Lambda^{ei} - \frac{1}{2} \right) + \frac{4(\gamma+1)^2}{\left[2^{\sqrt{(\gamma+1)/2}} \right]^4} Z \left(\ln \Lambda^{ee} - \frac{1}{2} \right) \right\}. \quad (8)$$

κ_1 is related to the slowing-down cross section,² which characterizes the loss of directed velocity in the scattering, and κ_2 is related to the deflection cross section, which represents the mean-square increment in the transverse electron velocity during the scattering process.² $\beta = v/c$ and $\gamma = (1 - \beta^2)^{-1/2}$; $r_0 = e^2/m_0c^2$ is the classical electron radius. The appropriate Coulomb logarithms are evaluated in an earlier paper.¹⁴ The angular distribution function is obtained from

$$\begin{aligned}
 f(\theta, E) &= \frac{1}{4\pi} \sum_{\ell=0}^{\infty} (2\ell+1) P_{\ell}(\cos\theta) \\
 &\times \exp \left[- \int_{E_0}^E \kappa_{\ell}(E') \left(\frac{dE'}{ds} \right)^{-1} dE' \right], \quad (9)
 \end{aligned}$$

from which $\langle P_{\ell}(\cos\theta) \rangle$ is calculated:

$$\langle P_{\ell}(\cos\theta) \rangle = \exp \left[- \int_{E_0}^E \kappa_{\ell}(E') \left(\frac{dE'}{ds} \right)^{-1} dE' \right], \quad (10)$$

where dE/ds is plasma stopping power taken from Ref. 14. From these results, Eqs. (2) and (3) are solved, and basic moments required for the calculation of the longitudinal and lateral distributions are evaluated:

$$\langle x \rangle = \int_{E_0}^E \langle P_1(\cos\theta) \rangle \left(\frac{dE'}{ds} \right)^{-1} dE', \quad (11)$$

which was evaluated in previous work for the case of 1-MeV electron stopping in a 300-g/cm³ DT plasma at 5 keV. This results in a penetration of 13.9 μm (Ref. 14). For astrophysical jets, however, for which $n_e \sim 10/\text{cm}^3$, the penetration is $\sim 10^4$ light years:

$$\begin{aligned} \langle x^2 \rangle &= \frac{2}{3} \int_{E_0}^E \langle P_1(\cos\theta) \rangle \left(\frac{dE'}{ds} \right)^{-1} \\ &\times \left[\int_{E_0}^{E'} \frac{1 + 2 \langle P_2(\cos\theta) \rangle}{\langle P_1(\cos\theta) \rangle} \left(\frac{dE''}{ds} \right)^{-1} dE'' \right] dE', \quad (12) \end{aligned}$$

because of azimuthal symmetry,

$$\langle y \rangle = \langle z \rangle = 0, \quad (13)$$

and

$$\begin{aligned} \langle y^2 \rangle = \langle z^2 \rangle &= \frac{2}{3} \int_{E_0}^E \langle P_1(\cos\theta) \rangle \left(\frac{dE'}{ds} \right)^{-1} \\ &\times \left[\int_{E_0}^{E'} \frac{1 - \langle P_2(\cos\theta) \rangle}{\langle P_1(\cos\theta) \rangle} \left(\frac{dE''}{ds} \right)^{-1} dE'' \right] dE'. \quad (14) \end{aligned}$$

Range or longitudinal straggling is defined by

$$\Sigma_R(E) = \sqrt{\langle x^2 \rangle - \langle x \rangle^2}. \quad (15)$$

Beam blooming is defined by

$$\Sigma_B(E) = \sqrt{\langle y^2 \rangle}. \quad (16)$$

Figure 102.30 shows the calculated straggling [Fig. 102.30(a)] and blooming [Fig. 102.30(b)] that result from the effects of scattering off electrons alone and off electrons plus ions. Energy deposition, toward the end of the penetration, is transferred to an extended region about the mean penetration of 13.8 μm , specifically $\sim \pm 3 \mu\text{m}$ longitudinally and $\sim \pm 5 \mu\text{m}$ laterally. From a different point of view, Fig. 102.31 shows the

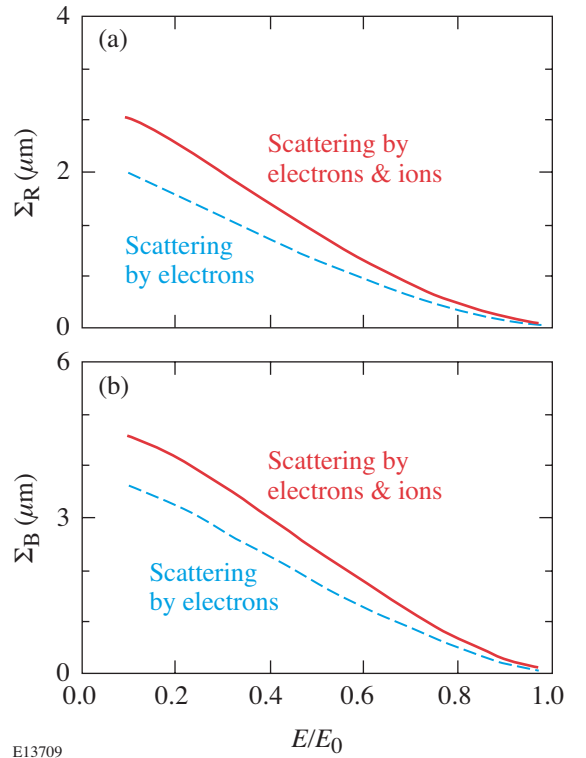


Figure 102.30
For 1-MeV electrons in a DT plasma ($\rho = 300 \text{ g/cm}^3$, $T_e = 5 \text{ keV}$): (a) The calculated range straggling $\Sigma_R(E)$ and (b) lateral blooming $\Sigma_B(E)$ are plotted as functions of electron residual energy. For this case, the penetration $\langle x \rangle$ is 13.9 μm (Ref. 14).

enhancement of the stopping power in the extended region in which longitudinal straggling is important. Including the effects of blooming would effectively increase (decrease) Σ_R for values less (greater) than the mean penetration.

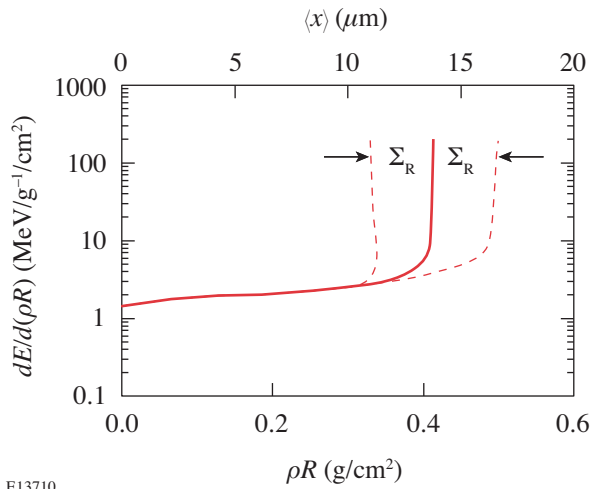


Figure 102.31 The stopping power, plotted as a function of the electron penetration. The solid line represents the mean energy loss, while the two dashed lines indicate the straggling range over which energy is effectively spread (in this plot, important contributions from blooming are not included; see text). As a result of the scattering, the energy transfer increases notably near the end of the penetration (i.e., an effective Bragg peak).

Figure 102.32 shows the effects of both straggling and blooming as a function of the square root of the penetration. Note that little straggling or blooming occurs until the 1-MeV electrons have traversed a significant portion of the final penetration (~60%, corresponding to only ~40% energy loss). Therefore, the assumption of uniform energy deposition, used in some previous calculations,¹¹ has some approximate justification for only the first ~40% of the energy loss. For energy loss greater than 40%, both straggling and blooming expand linearly with the square root of the penetration, an effect associated with the enhanced energy loss of the effective Bragg peak (Fig. 102.31). As a direct consequence of these multiple scattering effects, these results demonstrate the inextricable linkage between enhanced energy loss, straggling, and blooming.

Figure 102.33 shows a schematic representation of an FI capsule. The relativistic electrons are generated by an intense laser interacting at the critical surface. As the electrons are initially generated and transported, they are subject to Weibel-like instabilities,^{20,21} which can cause both spreading and

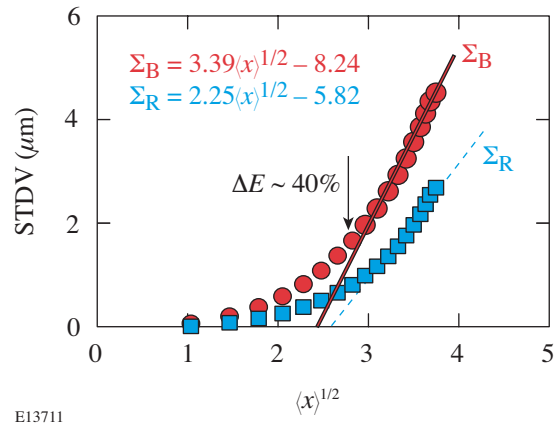


Figure 102.32 The longitudinal range straggling and lateral blooming of a 1-MeV electron beam, plotted as a function of the square root of the penetration ($\langle x \rangle$), for conditions of Fig. 102.30. Note that when the electrons have lost more than ~40% of their energy, both Σ_R and Σ_B are approximately proportional to $\sqrt{\langle x \rangle}$. Equations listed in the figure are the results of fitting only this final portion of the penetration.

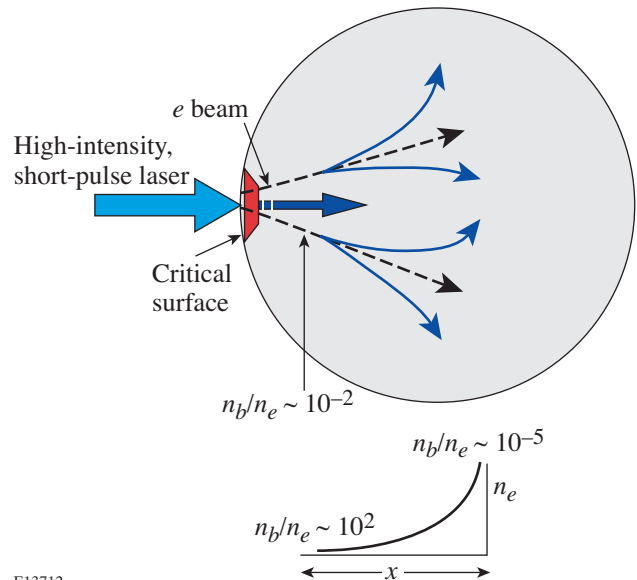


Figure 102.33 Schematic illustration of beam blooming in a precompressed FI capsule. Two distinct regions for electron transport are illustrated: first, when $n_b/n_e > 10^{-2}$, the electron transport is highly filamented due to Weibel-like instabilities that dominate energy loss and beam blooming; however, for $n_b/n_e < 10^{-2}$, which occurs as the beam penetrates farther into the denser portion of the capsule, Weibel-like instabilities are stabilized and the electrons are then subject to the multiple scattering, straggling, and blooming processes described herein. The dashed lines schematically indicate electron-beam trajectories without the effects of multiple scattering blooming and straggling (see text).

energy loss in this region. However, for electrons that transport farther into the increased-density portions of the capsule $n_b/n_e < 10^{-2}$, Weibel-like instabilities are stabilized and the electrons then become subject to the multiple scattering processes described herein. In this regime, the interaction can be envisioned as the linear superposition of individual, isolated electrons interacting with plasma. Therefore, these scattering processes, which involve energy loss, straggling, and beam blooming, become the ultimate mechanism that determines the details of energy deposition, whether in the dense core or outside, and ultimately determine the effectiveness of capsule ignition. From a different point of view, the extent of beam blooming and straggling is critical for FI target design since the finite size of the highly compressed core requires accurate understanding and control of beam divergence, which, if too severe, will preclude ignition.

In summary, from fundamental principles, the interaction of directed energetic electrons with hydrogenic plasmas is analytically modeled. For the first time, the effects of stopping, straggling, and beam blooming—a consequence of multiple scattering and energy loss—are rigorously treated from a unified approach. For fast ignition, enhanced energy deposition is found to be inextricably linked to beam blooming and straggling. We demonstrate that the mutual interaction of these effects will lead to an enhanced nonuniform region of energy deposition. Blooming and straggling effects will eventually dominate over all other sources of beam divergence and are therefore critical for evaluating the requirements of fast ignition.

ACKNOWLEDGMENT

This work was supported in part by U.S. Department of Energy Contract #DE-FG03-99SF21782, LLE subcontract #PO410025G, LLNL subcontract #B313975, and the Fusion Science Center for Extreme States of Matter and Fast Ignition Physics at University of Rochester.

REFERENCES

1. L. Spitzer, *Physics of Fully Ionized Gases*, 2nd rev. ed., Interscience Tracts on Physics and Astronomy (Interscience, New York, 1962).
2. B. A. Trubnikov, in *Reviews of Plasma Physics*, edited by M. A. Leontovich (Consultants Bureau, New York, 1965).
3. C. K. Li and R. D. Petrasso, *Phys. Rev. Lett.* **70**, 3063 (1993).
4. J. D. Lindl, *Inertial Confinement Fusion: The Quest for Ignition and Energy Gain Using Indirect Drive* (Springer-Verlag, New York, 1998).
5. J. D. Lindl, R. L. McCrory, and E. M. Campbell, *Phys. Today* **45**, 32 (1992).
6. S. Skupsky, *Phys. Rev. A* **16**, 727 (1977).
7. C. K. Li and R. D. Petrasso, *Phys. Rev. Lett.* **70**, 3059 (1993).
8. R. D. Petrasso, J. A. Frenje, C. K. Li, F. H. Séguin, J. R. Rygg, B. E. Schwartz, S. Kurebayashi, P. B. Radha, C. Stoeckl, J. M. Soures, J. Delettrez, V. Yu. Glebov, D. D. Meyerhofer, and T. C. Sangster, *Phys. Rev. Lett.* **90**, 095002 (2003); V. A. Smalyuk, P. B. Radha, J. A. Delettrez, V. Yu. Glebov, V. N. Goncharov, D. D. Meyerhofer, S. P. Regan, S. Roberts, T. C. Sangster, J. M. Soures, C. Stoeckl, J. A. Frenje, C. K. Li, R. D. Petrasso, and F. H. Séguin, *Phys. Rev. Lett.* **90**, 135002 (2003); F. H. Séguin, J. A. Frenje, C. K. Li, D. G. Hicks, S. Kurebayashi, J. R. Rygg, B.-E. Schwartz, R. D. Petrasso, S. Roberts, J. M. Soures, D. D. Meyerhofer, T. C. Sangster, J. P. Knauer, C. Sorce, V. Yu. Glebov, C. Stoeckl, T. W. Phillips, R. J. Leeper, K. Fletcher, and S. Padalino, *Rev. Sci. Instrum.* **74**, 975 (2003); J. A. Frenje, C. K. Li, and F. H. Séguin, *Phys. Plasmas* **11**, 2798 (2004).
9. M. Tabak *et al.*, *Phys. Plasmas* **1**, 1626 (1994).
10. C. Deutsch *et al.*, *Phys. Rev. Lett.* **77**, 2483 (1996); **85**, 1140 (E) (2000).
11. S. Atzeni, *Phys. Plasmas* **6**, 3316 (1999).
12. M. H. Key, M. D. Cable, T. E. Cowan, K. G. Estabrook, B. A. Hammel, S. P. Hatchett, E. A. Henry, D. E. Hinkel, J. D. Kilkenny, J. A. Koch, W. L. Kruer, A. B. Langdon, B. F. Lasinski, R. W. Lee, B. J. MacGowan, A. MacKinnon, J. D. Moody, M. J. Moran, A. A. Offenberger, D. M. Pennington, M. D. Perry, T. J. Phillips, T. C. Sangster, M. S. Singh, M. A. Stoyer, M. Tabak, G. L. Tietbohl, M. Tsukamoto, K. Wharton, and S. C. Wilks, *Phys. Plasmas* **5**, 1966 (1998).
13. C. Ren *et al.*, *Phys. Rev. Lett.* **93**, 185004 (2004).
14. C. K. Li and R. D. Petrasso, *Phys. Rev. E* **70**, 067401 (2004).
15. M. D. Rosen *et al.*, *Phys. Rev. A* **36**, 247 (1987).
16. P. A. Hughes, ed. *Beams and Jets in Astrophysics*, Cambridge Astrophysics Series (Cambridge University Press, Cambridge, England, 1991).
17. H. W. Lewis, *Phys. Rev.* **78**, 526 (1950).
18. N. F. Mott, *Proc. R. Soc. Lond. A, Math. Phys. Sci.* **A124**, 425 (1929); N. F. Mott, M. A. Gonville, and C. College, *Proc. R. Soc. Lond. A, Math. Phys. Sci.* **CXXXV**, 429 (1932).
19. Chr. Møller, *Ann. Phys.* **14**, 531 (1932).
20. E. S. Weibel, *Phys. Rev. Lett.* **2**, 83 (1959).
21. M. Honda, J. Meyer-ter-Vehn, and A. Pukhov, *Phys. Rev. Lett.* **85**, 2128 (2000).